Topological Invariant for Bosonic Bogoliubov-de Gennes Systems with Disorder

Yutaka Akagi

Department of Physics, Graduate School of Science, The University of Tokyo, Hongo, Tokyo 113-0033, Japan (Dated: October 16, 2020)

Using the method of noncommutative geometry, we define a topological invariant in disordered bosonic Bogoliubov-de Gennes systems, which possess a unique mathematical property—non-Hermiticity. To demonstrate the validity of the definition, we investigate a disordered artificial spin ice model in two dimensions numerically. In the clean limit, we clarify that the topological index perfectly coincides with the Chern number. We also show that the topological index is robust against disorder. The formula provides the topological index $n_{\rm Ch}=1$ in the magnon Hall regime and $n_{\rm Ch}=0$ in a trivial localized one. We also show by example that our method can be extended to other symmetry classes. Our results pave the way for further studies on topological bosonic systems with disorder.

In recent decades, the classification of topological insulators/superconductors and the related phenomena have been studied intensively [1–5]. Nontrivial topology in materials usually results in the appearance of robust edge states, which are also expected to provide potential applications [6–8]. Such nontrivial phases are characterized by certain topological invariants. A well-known example is the Chern number, which corresponds one-to-one with the number of chiral edge states in a quantum Hall system, known as the bulk-boundary correspondence [9, 10].

It has been realized that bosonic systems also exhibit topological phenomena, such as the topological (thermal) Hall effect. Examples range from systems of photons [11– 16], to systems of phonons [17–25], magnons [26–48], and triplons [49, 50]. Among the various bosonic systems, research on topological aspects of magnonic systems has increased rapidly. Recently, it has also been found that magnonic systems provide symmetry-protected topological phases, for instance, the \mathbb{Z}_2 topological phases [51– 53] and higher-order topological phases [54, 55]. As a difference from fermionic systems, bosonic Bogoliubovde Gennes (BdG)-type systems, which contain pairing terms, possess non-Hermicity intrinsically due to the bosonic statistics. Therefore, the topological classification of Hermitian systems is not directly applicable to bosonic BdG systems [56, 57].

Topological phases are expected to be robust against disorder owing to their topological nature. However, it is not obvious how to define topological invariants in the presence of disorder due to broken translational symmetry. Recently, it was found that the approach of noncommutative geometry [58–60] provides mathematically rigorous representations of topological invariants for the ten Altland-Zirnbauer classes [61]. The numerical method for calculating the invariants has been established as well [62]. Various other expressions within the symmetry classes have also been defined, such as the Chern number in real space [63–65] and the Bott index [66–71].

However, a numerical determination of the topological index for bosonic BdG systems with disorder is still

very challenging. Roughly speaking, two methods have been proposed so far for this problem: the C^* -algebraic approach [72] and the consctruction of the real-space Bott index [73]. In this paper, we propose an alternative and highly efficient method to numerically calculate the topological index for magnon Hall systems with disorder. The method is based on the noncommutative index theory [58–60, 62] and has an advantage in that the extension of the method to other symmetry classes is straightforward. Some examples are given at the end of the paper.

Our method is demonstrated for the artificial spin ice model with disorder, which exhibits the magnon Hall effect [74]. As in fermionic systems, the noncommutative index in the clean limit perfectly coincides with the conventional Chern number [33] corresponding to the number of chiral edge states. We also show that the topological index is robust against disorder, and the index $n_{\rm Ch} = 1$ (0) characterizes the disordered topological (a trivial localized) magnon phase.

We begin with the bosonic BdG Hamiltonian

$$\mathcal{H}_{\mathrm{BdG}} = \frac{1}{2} \sum_{k} \beta^{\dagger} H_{\mathrm{BdG}} \beta, \tag{1}$$

$$\boldsymbol{\beta}^{\dagger} = [b_1^{\dagger}, \cdots, b_{\mathscr{N}}^{\dagger}, b_1, \cdots, b_{\mathscr{N}}].$$
 (2)

Here, $b_j^{\dagger}\left(b_j\right)$ denotes boson creation (annihilation) operator with label j. The subscript $\mathscr N$ is the total number of degrees of freedom in a system (in this paper, the $\mathscr N$ is the total number of sites). The matrix H_{BdG} is written as

$$H_{\text{BdG}} = \begin{pmatrix} h & \Delta \\ \Delta^* & h^* \end{pmatrix}. \tag{3}$$

Since the $2\mathcal{N} \times 2\mathcal{N}$ matrix H_{BdG} is Hermitian, the $\mathcal{N} \times \mathcal{N}$ matrices h and Δ satisfy $h^{\dagger} = h$ and $\Delta^T = \Delta$, respectively. Here, O^* , O^{\dagger} , and O^T are the complex conjugate, adjoint, and transposition of a matrix O, respectively. The components of the operator $\boldsymbol{\beta}$ satisfy

the commutation relation $[\beta_i, \beta_j^{\dagger}] = (\Sigma_z)_{ij}$. Here, Σ_z is defined as a tensor product $\Sigma_a := \sigma_a \otimes 1_{\mathscr{N}}$, where σ_a (a = x, y, z) is the a-component of the Pauli matrix acting on the particle-hole space and $1_{\mathscr{N}}$ is the $\mathscr{N} \times \mathscr{N}$ identity matrix.

To hold the bosonic commutation relation, the Hamiltonian H_{BdG} is diagonalized by a para-unitary matrix T, which satisfies $T^{\dagger}\Sigma_z T = \Sigma_z$. Solving the eigenvalue problem $\Sigma_z H_{\text{BdG}} \boldsymbol{v}_j = E_j \boldsymbol{v}_j$, we obtain the eigenvalues E_j of H_{BdG} and the para-unitary matrix (eigenvectors \boldsymbol{v}_j) automatically:

$$T^{-1}\Sigma_z H_{\text{BdG}}T = \text{diag}[E_1, \cdots, E_{\mathcal{N}}, -E_1, \cdots, -E_{\mathcal{N}}],$$
(4)

where the para-unitary matrix is given by

$$T = [\mathbf{v}_1, \cdots, \mathbf{v}_{\mathcal{N}}, \mathbf{v}_{\mathcal{N}+1}, \cdots, \mathbf{v}_{2\mathcal{N}}]. \tag{5}$$

Since the effective Hamiltonian $\Sigma_z H_{\rm BdG}$ is non-Hermitian, the inner-product for bosonic wave functions is modified as

$$\langle\!\langle \boldsymbol{\phi}, \boldsymbol{\psi} \rangle\!\rangle = \boldsymbol{\phi}^{\dagger} \Sigma_z \boldsymbol{\psi}, \tag{6}$$

where ϕ and ψ are $2\mathcal{N}$ -dimensional complex vectors [75].

Next, for defining the topological invariant, we introduce a "Fermi" projection $P_{\rm B}$ for bosonic BdG systems described by

$$P_{\rm B} = \frac{1}{2\pi i} \oint_{\mathcal{C}} (z - \Sigma_z \mathcal{H}_{\rm BdG})^{-1} dz$$
$$= \sum_{E_n \le E_{\rm B}} (\Sigma_z)_{nn} v_n v_n^{\dagger} \Sigma_z, \tag{7}$$

where the contour \mathcal{C} encloses all the spectrum of $\Sigma_z \mathcal{H}_{\mathrm{BdG}}$ below the "Fermi" energy for bosons E_{B} . As in fermionic systems, the P_{B} is the projection onto the states whose energies are less than the fictitious Fermi energy E_{B} . The element of Eq. (7) $P_n := (\Sigma_z)_{nn} v_n v_n^{\dagger} \Sigma_z$ satisfies $P_m P_n = \delta_{mn} P_n$ (i.e., $P_{\mathrm{B}}^2 = P_{\mathrm{B}}$) and $\sum_{n=1}^{2\mathcal{N}} P_n = 1_{2\mathcal{N}}$, and thus the effective Hamiltonian is rewritten as $\Sigma_z H_{\mathrm{BdG}} = \sum_n E_n P_n$ (spectral decomposition). We note that the projection P_n is no longer Hermitian as the operator satisfies $\Sigma_z P_n^{\dagger} \Sigma_z = P_n$.

As in fermionic systems, we also introduce the Dirac operator $\tilde{\mathcal{D}}_a$ for bosonic BdG systems as

$$\tilde{\mathcal{D}}_{\boldsymbol{a}} := \sigma_z \otimes \mathcal{D}_{\boldsymbol{a}}(\boldsymbol{x}), \ \mathcal{D}_{\boldsymbol{a}}(\boldsymbol{x}) := \frac{x + iy - (a_x + ia_y)}{|x + iy - (a_x + ia_y)|}.$$
 (8)

Here, $\mathbf{x} = (x, y)$ is the position vector of lattice points, and $\mathbf{a} = (a_x, a_y) \neq \mathbf{x}$ is a vector of a flux point [see Fig. 1(a)].

Next, we define the topological index for tight-binding models of bosonic BdG systems with disorder. The dif-

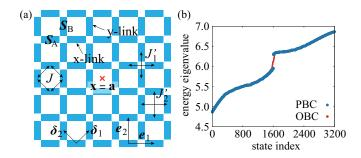


FIG. 1. (Color online). (a) Artificial spin ice model on a square lattice with the nearest (next nearest) neighbor dipole coupling J (J_1' and J_2'). A(B)-sublattice spins $\mathbf{S}_{i\in A}$ ($\mathbf{S}_{i\in B}$) are located on the center of the x(y)-link. We define vectors in Eq. (17) as $e_1=(1,0),\ e_2=(0,1),\ \delta_1=(1/2,1/2),$ and $\delta_2=(-1/2,1/2).$ The location of \boldsymbol{a} in Eq. (8) is chosen to be the center of the lattice. (b) Magnon energy spectrum of Eq. (17) in the clean limit with PBC and OBC. The topological edge state shown in red traverses the energy gap with PBC between 5.96 and 6.30. The parameters used in (b) are $J=1.0,\ J_1'=J_2'=0.35,\ D=2.0,\ H^z=20.0,\ S=1.0$ and the system size is $L^2=3200$.

ference of two projections is defined as [58, 59]

$$A := P_{\mathbf{B}} - \tilde{\mathcal{D}}_{\mathbf{a}}^{\dagger} P_{\mathbf{B}} \tilde{\mathcal{D}}_{\mathbf{a}} \tag{9}$$

where $\tilde{\mathcal{D}}_{a}^{\dagger}$ is the adjoint of the Dirac operator $\tilde{\mathcal{D}}_{a}$. Suppose that A^{2n+1} for $n \in \mathbb{N}$ is trace class. Then, the topological index n_{Ch} is defined as

$$n_{\text{Ch}} := \dim \ker [A-1] - \dim \ker [A+1],$$
 (10)

where dim ker O stands for the dimension of the kernel of an operator O. We note two properties of the operator A: (i) ||A|| < 1 since the operator A consists of the difference between two projections. (ii) The eigenvalues of the non-Hermitian operator A are real because of the relation $\Sigma_z A^{\dagger} \Sigma_z = A$, which is derived from $\Sigma_z P_n^{\dagger} \Sigma_z = P_n$.

We here show the underlying supersymmetric structure of the operator A. According to Refs. [58, 59], a pair operator of A is defined as

$$B := 1 - P_{\mathcal{B}} - \tilde{\mathcal{D}}_{\boldsymbol{a}}^{\dagger} P_{\mathcal{B}} \tilde{\mathcal{D}}_{\boldsymbol{a}}. \tag{11}$$

The operators A and B satisfy the following two relations:

$$AB + BA = 0$$
 and $A^2 + B^2 = 1$. (12)

Let φ_1 be an eigenvector of A with an eigenvalue λ , i.e., $A\varphi_1 = \lambda \varphi_1$. Then, the anti-commutation relation of Eq. (12) yields

$$AB\varphi_1 = -BA\varphi_1 = -\lambda B\varphi_1. \tag{13}$$

The second relation of Eq. (12) produces

$$B^2 \varphi_1 = (1 - \lambda^2) \varphi_1$$
 and $\langle \langle B\varphi_1, B\varphi_1 \rangle \rangle = (1 - \lambda^2) \langle \langle \varphi_1, \varphi_1 \rangle \rangle,$ (14)

where we used $\Sigma_z B^{\dagger} \Sigma_z = B$, which is also derived from $\Sigma_z P_n^{\dagger} \Sigma_z = P_n$. Equations (13) and (14) imply that B is an invertible map from an eigenvector with an eigenvalue λ to that with $-\lambda$, except for $\lambda = 0, \pm 1$. In other words, λ and $-\lambda$ for $0 < |\lambda| < 1$ always come in pairs while $\lambda = \pm 1$ are isolated points of the spectrum of A [76].

Let us consider the robustness of the index against a perturbation $\delta \mathcal{H}_{BdG}$ as discussed in Refs. [61, 77]. The projection for the total Hamiltonian $\mathcal{H}'_{BdG} := \mathcal{H}_{BdG} + \delta \mathcal{H}_{BdG}$ is written as

$$P_{\rm B}' = \frac{1}{2\pi i} \oint_{\mathcal{C}} (z - \Sigma_z \mathcal{H}'_{\rm BdG})^{-1} dz, \tag{15}$$

and then we introduce $A' := P'_{\rm B} - \tilde{\mathcal{D}}_{\bf a}^{\dagger} P'_{\rm B} \tilde{\mathcal{D}}_{\bf a}$ as the A operator for $\mathcal{H}'_{\rm BdG}$. We here consider the following two assumptions: (i) The range of the hopping integrals of $\delta\mathcal{H}_{\rm BdG}$ is finite, i.e., the norm $\|\delta\mathcal{H}_{\rm BdG}\|$ is finite. (ii) The fictitious Fermi level for bosons still lies in the spectral gap of $\mathcal{H}'_{\rm BdG}$. Using the contour integral, we write the difference between $P'_{\rm B}$ and $P_{\rm B}$ as

$$P_{\rm B}' - P_{\rm B} = \frac{1}{2\pi i} \oint_{\mathcal{C}} \frac{1}{z - \Sigma_z \mathcal{H}_{\rm BdG}'} \Sigma_z \delta \mathcal{H}_{\rm BdG} \frac{1}{z - \Sigma_z \mathcal{H}_{\rm BdG}} dz. \quad (16)$$

Because of the spectral gap assumption, the norm of the right-hand side can be bounded by the norm $\|\Sigma_z \delta \mathcal{H}_{BdG}\|$. Then, the difference $A' - A = (P'_B - P_B) - \tilde{\mathcal{D}}_a^{\dagger}(P'_B - P_B)\tilde{\mathcal{D}}_a$ is bounded by the norm, and thus the operator A is continuous with respect to $\|\Sigma_z \delta \mathcal{H}_{BdG}\|$. Using the Weyl's inequality for the real spectrum [78], we obtain the desired results that the nonzero eigenvalue λ of the operator A is continuous with respect to $\|\Sigma_z \delta \mathcal{H}_{BdG}\|$ [see the spectrum in red regions of Fig. 2 as we discuss later in detail]. Consequently, the topological index given by Eq. (10) is robust against perturbations.

As a demonstration, we compute the topological index n_{Ch} of the disordered artificial spin ice model on a square lattice, which exhibits the magnon Hall effect [refer to the original spin Hamiltonian in Ref. [74]]. In this model, A(B)-sublattice spin on x(y)-link of the square lattice has an easy-axis anisotropy D_j along the x(y)-direction due to a magnetic shape anisotropy [79–82] [see Fig. 1(a)]. We here consider a fully polarized state by the out-of-plane strong magnetic field H_j^z . By applying the Holstein-Primakoff transformation, the magnon Hamil-

tonian of the model is written as

$$H_{\text{BdG}} := H_{\text{on}} + H_{\text{nn}} + H_{\text{nnn}}$$

$$H_{\text{on}} = \frac{1}{2} \sum_{j \in A} \left\{ (D + d_{j}) S(-b_{j}^{\dagger 2} - b_{j}^{\dagger} b_{j}) + (H^{z} + h_{j}) b_{j}^{\dagger} b_{j} \right\}$$

$$+ \frac{1}{2} \sum_{j \in B} \left\{ (D + d_{j}) S(b_{j}^{\dagger 2} - b_{j}^{\dagger} b_{j}) + (H^{z} + h_{j}) b_{j}^{\dagger} b_{j} \right\} + \text{h.c.}$$

$$H_{\rm nn} \equiv \sum_{m=1,2} \sum_{\boldsymbol{j} \in A} \sum_{\boldsymbol{i} = \boldsymbol{j} \pm \delta_m, \boldsymbol{i} \in B} \frac{JS}{2} \left(-b_{\boldsymbol{j}}^{\dagger} b_{\boldsymbol{i}} - b_{\boldsymbol{i}}^{\dagger} b_{\boldsymbol{i}} - b_{\boldsymbol{j}}^{\dagger} b_{\boldsymbol{j}} + 3i(-1)^m b_{\boldsymbol{j}}^{\dagger} b_{\boldsymbol{i}}^{\dagger} + \text{h.c.} \right)$$

$$H_{\rm nnn} \equiv \sum_{\alpha = A,B} \sum_{m=1,2} \sum_{\boldsymbol{j} \in \alpha} \sum_{\boldsymbol{i} = \boldsymbol{j} \pm e_m} \frac{J'_{\alpha,m} S}{4} \left(-b_{\boldsymbol{j}}^{\dagger} b_{\boldsymbol{i}} - b_{\boldsymbol{i}}^{\dagger} b_{\boldsymbol{i}} - b_{\boldsymbol{j}}^{\dagger} b_{\boldsymbol{j}} + 3(-1)^m b_{\boldsymbol{j}}^{\dagger} b_{\boldsymbol{i}}^{\dagger} + \text{h.c.} \right),$$

$$(17)$$

where b_{j}^{\dagger} (b_{j}) is the magnon creation (annihilation) operator at site j, and S is the spin magnitude. The coupling constant J and $J'_{\alpha,m}$ denote the nearest and the next nearest dipolar interactions, respectively with $J'_{A,1} = J'_{B,2} = J'_{1}$ and $J'_{A,2} = J'_{B,1} = J'_{2}$. As shown in Fig. 1(a), e_{1} and e_{2} are the primitive lattice vectors of the square lattice and $\delta_{m} = [e_{1} - (-1)^{m} e_{2}]/2$ (m = 1, 2). The easy-axis anisotropy and magnetic field include randomness as $D_{j} = D + d_{j}$ and $H_{j}^{z} = H^{z} + h_{j}$ where D and H^{z} are uniform components. The randomness d_{j} and h_{j} are uniformly distributed within [-W/2, W/2] with a positive parameter W.

Figure 1(b) shows the magnon energy spectrum, in ascending order, of the model in the absence of disorder. The blue/red dots are the energy spectrum under periodic/open boundary condition (PBC/OBC). As shown in the figure, the topological edge state (OBC) traverses the energy gap between 5.96 and 6.30 (PBC). This is because the Chern number of the bottom (top) band is +1 (-1), which is computed in terms of the Bloch wave-function in crystal momentum space.

To evaluate the topological index, we plot $E_{\rm B}$ and W dependences of the eigenvalues λ_i (i=1,2,N-2,N-1,N) of the operator A as shown in Fig. 2 [see Ref. [62] for detailed numerical implementation]. Here, we write λ_i for the i-th eigenvalue of the operator A in ascending order, i.e., $(-1 \le)$ $\lambda_1 \le \lambda_2 \le \cdots \le \lambda_N$ (≤ 1). As shown in the red regions of Fig. 2(a) and (b), $\lambda_N \simeq 1$, $\lambda_1 \ne -1$, and $\lambda_N - \lambda_{N-1} \ne 0$, and hence $n_{\rm Ch} = 1$. The region of $n_{\rm Ch} = 1$ for W = 0.0 (absence of disorder) in Fig. 2(a) perfectly coincides with that with the Chern number +1. As discussed above, one can see the pairing structure as $\lambda_{N-1} \simeq -\lambda_1$ and $\lambda_{N-2} \simeq -\lambda_2$ in the red regions. One can also see, in the red regions, that the spectrum is continuous. On the other hand, in the white regions, the

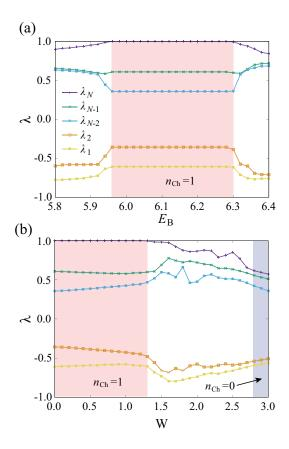


FIG. 2. (Color online). (a) Fictitious Fermi level $E_{\rm B}$ and (b) disorder strength W dependences of the eigenvalues λ_1 , λ_2 , λ_{N-2} , λ_{N-1} , and λ_N of the operator A. (a) and (b) correspond to cross-sections of Fig. 3 for W=0.0 and $E_{\rm B}=6.2$, respectively. The red (blue) colored region is the magnon Hall (trivial localized) regime characterized by $n_{\rm Ch}=1$ ($n_{\rm Ch}=0$). The parameters used in (a) and (b) are J=1.0, $J_1'=J_2'=0.35$, D=2.0, $H^z=20.0$, S=1.0 and the system size is $L^2=3200$.

spectrum fluctuates, and the pairing structure is broken. We note that our method is not effective because the spectral or mobility gap is expected to vanish in the white regions [62].

The blue region of Fig. 2(b) clearly shows the reconstruction of the pairing structure as $\lambda_N \simeq -\lambda_1$ and $\lambda_{N-1} \simeq -\lambda_2$. This implies that in the blue region, magnons are localized by disorder. In the localized regime, the eigenvalue λ_N is significantly different from unity, and thus $n_{\rm Ch} = 0$. From the observation of Fig. 2(a) and (b), we find that the largest (smallest) eigenvalue λ_N (λ_1) and the difference between λ_N and $|\lambda_1|$, i.e., $\lambda_N + \lambda_1$, give us information about the determination of the topological index $n_{\rm Ch}$.

Figure 3 represents $\lambda_N + \lambda_1$ as a function of the strength of disorder W and the fictitious Fermi level $E_{\rm B}$. In the blue region enclosed by the dotted line of Fig. 3, $\lambda_N > 0.995$ and $\lambda_N + \lambda_1 \simeq 0.4$, and hence $n_{\rm Ch} = 1$. In

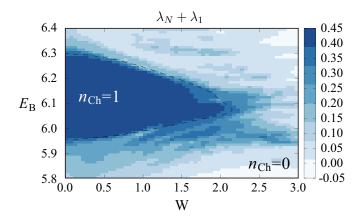


FIG. 3. (Color online). Dependence of $\lambda_N + \lambda_1$ with the topological index $n_{\rm Ch}$ in the artificial spin ice model as a function of the disorder strength W and the fictitious Fermi energy $E_{\rm B}$. The largest eigenvalue λ_N is larger than 0.995 in the blue region inside of the dotted line. The parameters are the same as in Fig. 2.

the localized regime of $\lambda_N + \lambda_1 \simeq 0$, the topological index $n_{\rm Ch}$ is zero as discussed in the Fig. 2(b). However, as in fermionic systems [62], it is difficult to identify the "metallic" phase, in which the spectral or mobility gap vanishes, only by the method of noncommutative geometry. It is beyond our scope of this paper to determine clear phase boundaries.

Summary: We have provided a new method for numerically calculating the topological index of magnon Hall systems with disorder. Introducing the "Fermi" projection for bosons $P_{\rm B}$, we have defined the topological index $n_{\rm Ch}$ determined by the discrete spectrum of the operator A with a supersymmetric structure. To check the validity of our method, we have computed the topological index for the artificial spin ice model with disorder [74]. As in fermionic systems [62], we have clarified that in the clean limit, the region with the topological index $n_{\rm Ch}=1$ perfectly coincides with that with the Chern number +1 corresponding to the number of chiral edge states. We have also shown that the index $n_{\rm Ch}=1$ (0) characterizes the disordered topological (trivial localized) magnon phase.

Finally, we remark that the generalization of our method to models in other symmetry classes is straightforward. For instance, the \mathbb{Z}_2 index ν in bosonic BdG systems with pseudo-time-reversal symmetry in two and three dimensions [52, 53, 57] is defined as

$$\nu = \dim \ker[A - 1] \mod 2, \tag{18}$$

as in fermionic systems [61, 62, 77]. Here, in two dimensions, the definition of the operator A is the same as Eq. (9). In three dimensions, the operator A is given by

$$A := P_B - \tilde{D}_a P_B \tilde{D}_a, \tag{19}$$

where the Dirac operator \tilde{D}_a is defined as

$$\tilde{D}_{a} := \sigma_{z} \otimes D_{a}(x), \ D_{a}(x) := \frac{1}{|x-a|}(x-a) \cdot \sigma(20)$$

Here, $\mathbf{x} = (x, y, z)$ is the position operator of lattices and $\mathbf{a} = (a_x, a_y, a_z) \neq \mathbf{x}$ is a vector of flux point as in Fig. 1(a). The vector $\boldsymbol{\sigma}$ is defined by $\boldsymbol{\sigma} = (\sigma_x, \sigma_y, \sigma_z)$. We will report the \mathbb{Z}_2 index ν in detail in a future article.

The author thanks Hosho Katsura for helpful discussions and for sharing his insights on the subject. The author also acknowledges useful discussions with Ken Shiozaki. This work was supported by JSPS KAK-ENHI Grants No. JP17K14352, JP20K14411, JSPS Grant-in-Aid for Scientific Research on Innovative Areas "Topological Materials Science" (KAKENHI Grant No. JP18H04220), and "Quantum Liquid Crystals" (KAK-ENHI Grant No. JP20H05154). The author also thanks the Okinawa Institute of Science and Technology Graduate University for the use of the facilities, Sango and Deigo clusters.

- A. P. Schnyder, S. Ryu, A. Furusaki, and A. W. W. Ludwig, Classification of topological insulators and superconductors in three spatial dimensions, Phys. Rev. B 78, 195125 (2008).
- [2] A. Kitaev, Periodic table for topological insulators and superconductors, AIP Conference Proceedings 1134, 22 (2009).
- [3] S. Ryu, A. P. Schnyder, A. Furusaki, and A. W. W. Ludwig, Topological insulators and superconductors: tenfold way and dimensional hierarchy, New J. Phys. 12, 065010 (2010).
- [4] M. Z. Hasan and C. L. Kane, Colloquium: Topological insulators, Rev. Mod. Phys. 82, 3045 (2010).
- [5] X.-L. Qi and S.-C. Zhang, Topological insulators and superconductors, Rev. Mod. Phys. 83, 1057 (2011).
- [6] A. Stern and N. H. Lindner, Topological Quantum Computation—From Basic Concepts to First Experiments, Science 339, 1179 (2013).
- [7] Z. Yue, G. Xue, J. Liu, Y. Wang, and M. Gu, Nanometric holograms based on a topological insulator material, Nat. Commun. 8, 15354 (2017).
- [8] Y. Zeng, U. Chattopadhyay, B. Zhu, B. Qiang, J. Li, Y. Jin, L. Li, A. G. Davies, E. H. Linfield, B. Zhang, Y. Chong, and Q. J. Wang, Electrically pumped topological laser with valley edge modes, Nature 578, 246 (2020).
- [9] Y. Hatsugai, Chern number and edge states in the integer quantum Hall effect, Phys. Rev. Lett. 71, 3697 (1993).
- [10] Y. Hatsugai, Edge states in the integer quantum Hall effect and the Riemann surface of the Bloch function, Phys. Rev. B 48, 11851 (1993).
- [11] M. Onoda, S. Murakami, and N. Nagaosa, Hall Effect of Light, Phys. Rev. Lett. 93, 083901 (2004).
- [12] O. Hosten and P. Kwiat, Observation of the Spin Hall Effect of Light via Weak Measurements, Science 319, 787 (2008).
- [13] S. Raghu and F. D. M. Haldane, Analogs of quantum-

- Hall-effect edge states in photonic crystals, Phys. Rev. A 78, 033834 (2008).
- [14] F. D. M. Haldane and S. Raghu, Possible Realization of Directional Optical Waveguides in Photonic Crystals with Broken Time-Reversal Symmetry, Phys. Rev. Lett. 100, 013904 (2008).
- [15] Z. Wang, Y. Chong, J. D. Joannopoulos, and M. Soljačić, Observation of unidirectional backscattering-immune topological electromagnetic states, Nature 461, 772 (2009).
- [16] P. Ben-Abdallah, Photon Thermal Hall Effect Phys. Rev. Lett. 116, 084301 (2016).
- [17] C. Strohm, G. L. J. A. Rikken, and P. Wyder, Phenomenological Evidence for the Phonon Hall Effect, Phys. Rev. Lett. 95, 155901 (2005).
- [18] L. Sheng, D. N. Sheng, and C. S. Ting, Theory of the Phonon Hall Effect in Paramagnetic Dielectrics, Phys. Rev. Lett. 96, 155901 (2006).
- [19] A. V. Inyushkin and A. N. Taldenkov, On the phonon Hall effect in a paramagnetic dielectric, JETP Lett. 86, 379 (2007).
- [20] Y. Kagan and L. A. Maksimov, Anomalous Hall Effect for the Phonon Heat Conductivity in Paramagnetic Dielectrics, Phys. Rev. Lett. 100, 145902 (2008).
- [21] J.-S. Wang and L. Zhang, Phonon Hall thermal conductivity from the Green-Kubo formula, Phys. Rev. B 80, 012301 (2009).
- [22] L. Zhang, J. Ren, J. -S. Wang, and B. Li, Topological Nature of the Phonon Hall Effect, Phys. Rev. Lett. 105, 225901 (2010).
- [23] T. Qin, J. Zhou, and J. R. Shi, Berry curvature and the phonon Hall effect, Phys. Rev. B, 86, 104305 (2012).
- [24] M. Mori, A. Spencer-Smith, O. P. Sushkov, and S. Maekawa, Origin of the Phonon Hall Effect in Rare-Earth Garnets, Phys. Rev. Lett. 113, 265901 (2014).
- [25] K. Sugii, M. Shimozawa, D. Watanabe, Y. Suzuki, M. Halim, M. Kimata, Y. Matsumoto, S. Nakatsuji, and M. Yamashita, Thermal Hall Effect in a Phonon-Glass Ba₃CuSb₂O₉, Phys. Rev. Lett. 118, 145902 (2017).
- [26] S. Fujimoto, Hall Effect of Spin Waves in Frustrated Magnets, Phys. Rev. Lett. 103, 047203 (2009).
- [27] H. Katsura, N. Nagaosa, and P. A. Lee, Theory of the Thermal Hall Effect in Quantum Magnets, Phys. Rev. Lett. 104, 066403 (2010).
- [28] Y. Onose, T. Ideue, H. Katsura, Y. Shiomi, N. Nagaosa, and Y. Tokura, Observation of the Magnon Hall Effect, Science 329, 297 (2010).
- [29] R. Matsumoto and S. Murakami, Theoretical Prediction of a Rotating Magnon Wave Packet in Ferromagnets, Phys. Rev. Lett. 106, 197202 (2011).
- [30] R. Matsumoto and S. Murakami, Rotational motion of magnons and the thermal Hall effect, Phys. Rev. B, 84, 184406 (2011).
- [31] T. Ideue, Y. Onose, H. Katsura, Y. Shiomi, S. Ishiwata, N. Nagaosa, and Y. Tokura, Effect of lattice geometry on magnon Hall effect in ferromagnetic insulators, Phys. Rev. B 85, 134411 (2012).
- [32] R. Shindou, J. I. Ohe, R. Matsumoto, S. Murakami, and E. Saitoh, *Chiral spin-wave edge modes in dipolar mag*netic thin films, Phys. Rev. B 87, 174402 (2013).
- [33] R. Shindou, R. Matsumoto, S. Murakami, and J. I. Ohe, Topological chiral magnonic edge mode in a magnonic crystal, Phys. Rev. B 87, 174427 (2013).
- [34] R. Matsumoto, R. Shindou, and S. Murakami, Thermal

- Hall effect of magnons in magnets with dipolar interaction, Phys. Rev. B 89, 054420 (2014).
- [35] A. Mook, J. Henk, and I. Mertig, Magnon Hall effect and topology in kagome lattices: A theoretical investigation, Phys. Rev. B 89, 134409 (2014).
- [36] R. Chisnell, J. S. Helton, D. E. Freedman, D. K. Singh, R. I. Bewley, D. G. Nocera, and Y. S. Lee, *Topological Magnon Bands in a Kagome Lattice Ferromagnet*, Phys. Rev. Lett. 115, 147201 (2015).
- [37] M. Hirschberger, Robin Chisnell, Young S. Lee, and N. P. Ong, Thermal Hall Effect of Spin Excitations in a Kagome Magnet, Phys. Rev. Lett. 115, 106603 (2015).
- [38] S. K. Kim, H. Ochoa, R. Zarzuela, and Y. Tserkovnyak, Realization of the Haldane-Kane-Mele Model in a System of Localized Spins, Phys. Rev. Lett. 117, 227201 (2016).
- [39] S. A. Owerre, A first theoretical realization of honeycomb topological magnon insulator, J. Phys.: Condens. Matter 28, 386001 (2016).
- [40] S. A. Owerre, Topological honeycomb magnon Hall effect: A calculation of thermal Hall conductivity of magnetic spin excitations, J. Appl. Phys. 120, 043903 (2016).
- [41] J. H. Han and H. Lee, Spin Chirality and Hall-Like Transport Phenomena of Spin Excitations, J. Phys. Soc. Jpn. 86, 011007 (2017).
- [42] S. Murakami and A. Okamoto, Thermal Hall Effect of Magnons, J. Phys. Soc. Jpn. 86, 011010 (2017).
- [43] K. Nakata, J. Klinovaja, and D. Loss, Magnonic quantum Hall effect and Wiedemann-Franz law, Phys. Rev. B 95, 125429 (2017).
- [44] X. S. Wang, Y. Su, and X. R. Wang, Topologically protected unidirectional edge spin waves and beam splitter, Phys. Rev. B 95, 014435 (2017).
- [45] X. S. Wang, H. W. Zhang, and X. R. Wang, Topological Magnonics: A Paradigm for Spin-Wave Manipulation and Device Design, Phys. Rev. Applied 9, 024029 (2018).
- [46] R. Seshadri and D. Sen, Topological magnons in a kagome-lattice spin system with XXZ and Dzyaloshinskii-Moriya interactions, Phys. Rev. B 97, 134411 (2018).
- [47] M. Kawano and C. Hotta, Thermal Hall effect and topological edge states in a square-lattice antiferromagnet, Phys. Rev. B 99, 054422 (2019).
- [48] S. K. Kim, K. Nakata, D. Loss, and Y. Tserkovnyak, Tunable Magnonic Thermal Hall Effect in Skyrmion Crystal Phases of Ferrimagnets, Phys. Rev. Lett. 122, 057204 (2019).
- [49] J. Rumhányi, K. Penc, and R. Ganesh, Hall effect of triplons in a dimerized quantum magnet, Nat. Commun. 6, 6805 (2015).
- [50] P. A. McClarty, F. Krüger, T. Guidi, S. F. Parker, K. Refson, A. W. Parker, D. Prabhakaran, and R. Coldea, Topological triplon modes and bound states in a Shastry-Sutherland magnet, Nat. Phys. 13, 736 (2017).
- [51] V. A. Zyuzin and A. A. Kovalev, Magnon Spin Nernst Effect in Antiferromagnets, Phys. Rev. Lett. 117, 217203 (2016).
- [52] H. Kondo, Y. Akagi, and H. Katsura, Z_2 topological invariant for magnon spin Hall systems, Phys. Rev. B **99**, 041110(R) (2019).
- [53] H. Kondo, Y. Akagi, and H. Katsura, Three-dimensional topological magnon systems, Phys. Rev. B 100, 144401 (2019).
- [54] T. Hirosawa, S. A. Díaz, J. Klinovaja, and D. Loss, Magnonic Quadrupole Topological Insulator in Antiskyrmion Crystals, Preprint arXiv:2005.05884 (2020).

- [55] A. Mook, S. A. Díaz, J. Klinovaja, and D. Loss, Chiral Hinge Magnons in Second-Order Topological Magnon Insulators, Preprint arXiv:2010.04142 (2020).
- [56] K. Kawabata, K. Shiozaki, M. Ueda, and M. Sato, Symmetry and Topology in Non-Hermitian Physics, Phys. Rev. X 9, 041015 (2019)
- [57] H. Kondo, Y. Akagi, and H. Katsura, Non-Hermiticity and topological invariants of magnon Bogoliubov-de Gennes systems, Preprint arXiv:2006.10391 (2020).
- [58] J. E. Avron, R. Seiler, and B. Simon, Charge Deficiency, Charge Transport and Comparison of Dimensions, Commun. Math. Phys. 159, 399 (1994).
- [59] J. Avron, R. Seiler, and B. Simon, The Index of a Pair of Projections, J. Func. Anal. 120, 220 (1994).
- [60] M. Aizenman, G. M. Graf, Localization Bounds for an Electron Gas, J. Phys. A31, 6783 (1998).
- [61] H. Katsura and T. Koma, The Noncommutative Index Theorem and the Periodic Table for Disordered Topological Insulators and Superconductors, J. Math. Phys. 59, 031903 (2018).
- [62] Y. Akagi, H. Katsura, and T. Koma, A New Numerical Method for Z₂ Topological Insulators with Strong Disorder, J. Phys. Soc. Jpn. 86, 123710 (2017).
- [63] A. Kitaev, Anyons in an exactly solved model and beyond, Ann. Phys. 321, 2 (2006).
- [64] E. Prodan, Robustness of the spin-Chern number, Phys. Rev. B 80, 125327 (2009).
- [65] E. Prodan, T. L. Hughes, and B. A. Bernevig, Entanglement Spectrum of a Disordered Topological Chern Insulator, Phys. Rev. Lett. 105, 115501 (2010).
- [66] J. Bellissard, A. van Elst, and H. Schulz Baldes, The noncommutative geometry of the quantum Hall effect, J. Math. Phys. 35, 5373 (1994).
- [67] M. B. Hastings and T. A. Loring, Almost commuting matrices, localized Wannier functions, and the quantum Hall effect, J. Math. Phys. 51, 015214 (2010).
- [68] T. A. Loring and M. B. Hastings, Disordered topological insulators via C*-algebras, EPL (Europhysics Lett.) 92, 67004 (2010).
- [69] T. A. Loring, K-theory and pseudospectra for topological insulators, Ann. Phys. 356, 383 (2015).
- [70] H. Huang and F. Liu, Quantum Spin Hall Effect and Spin Bott Index in a Quasicrystal Lattice, Phys. Rev. Lett. 121, 126401 (2018).
- [71] H. Huang and F. Liu, Theory of spin Bott index for quantum spin Hall states in nonperiodic systems, Phys. Rev. B 98, 125130 (2018).
- [72] V. Peano, H. Schulz-Baldes, Topological edge states for disordered bosonic systems, J. Math. Phys. 59, 031901 (2018).
- [73] X. S. Wang, A. Brataas, and R. E. Troncoso, Bosonic Bott Index and Disorder-Induced Topological Transitions of Magnons, Preprint arXiv:2006.16310 (2020).
- [74] B. Xu, T. Ohtsuki, and R. Shindou, Integer quantum magnon Hall plateau-plateau transition in a spin-ice model, Phys. Rev. B 94, 220403(R) (2016).
- [75] M. Lein and K. Sato, Krein-Schrödinger formalism of bosonic Bogoliubov-de Gennes and certain classical systems and their topological classification, Phys. Rev. B 100, 075414 (2019).
- [76] The supersymmetry structure produces Eq. (10) as $\operatorname{Tr} A^{2n+1} = \sum_{\lambda>0} \lambda^{2n+1} n_{\lambda} + (-\lambda)^{2n+1} n_{-\lambda} = n_1 n_{-1} = n_{\text{Ch}}$, where n_{λ} denotes the multiplicity of λ . Here, we used Lidskii's theorem. [83]

- [77] H. Katsura and T. Koma, The Z_2 index of disordered topological insulators with time reversal symmetry, J. Math. Phys. **57**, 021903 (2016).
- [78] R. Bhatia, Perturbation Bounds for Matrix Eigenvalues, (Society for Industrial and Applied Mathematics, 2007).
- [79] R. F. Wang, C. Nisoli, R. S. Freitas, J. Li, W. Mc-Conville1, B. J. Cooley, M. S. Lund, N. Samarth, C. Leighton, V. H. Crespi and P. Schiffer, Artificial 'spin ice' in a geometrically frustrated lattice of nanoscale ferromagnetic islands, Nature 439, 303 (2006).
- [80] Z. Budrikis, P. Politi, and R. L. Stamps, Vertex Dynamics in Finite Two-Dimensional Square Spin Ices, Phys.

- Rev. Lett. 105, 017201 (2010).
- [81] Z. Budrikis, J. P. Morgan, J. Akerman, A. Stein, P. Politi, S. Langridge, C. H. Marrows, and R. L. Stamps, Disorder Strength and Field-Driven Ground State Domain Formation in Artificial Spin Ice: Experiment, Simulation, and Theory, Phys. Rev. Lett. 109, 037203 (2012).
- [82] E. Iacocca, S. Gliga, R. L. Stamps, and O. Heinonen, Reconfigurable wave band structure of an artificial square ice, Phys. Rev. B, 93, 134420 (2016).
- [83] B. Simon, Trace Ideals and their Applications, (Cambridge University Press, Cambridge, 1979).